A Single-Gallery Model for the In Situ Production of Polyethylene-Clay Nanocomposites

*Abolfazl Maneshi, João B. P. Soares, Leonardo C. Simon**

Polyolefin-clay nanocomposites are finding many new applications because of their improved properties, such as high modulus, elevated scratch resistance and low gas permeability. Currently, these composites are produced by melt blending organically modified clay with polyolefins. The most challenging step in this process is the intercalation and exfoliation of the clay to produce a homogenously dispersed phase at the nanoscale. A promising alternative to melt blending is in-situ polymerization, where the polymer is produced between the clay layers in the polymerization reactor. In-situ polymerization of olefins with metallocene catalysts supported on clay can produce nanocomposites using conventional polymerization reactors, provided that the clay can be used as a support for the olefin polymerization catalyst. In this approach, the clay fulfills the functions of catalyst support and dispersed phase in the final nanocomposite. In this work, a mathematical model describing particle growth during in-situ polymerization of ethylene with a metallocene catalyst supported on clay will be discussed. The model expands the approach of the multi-grain model used in heterogeneous olefin polymerization to account for the layered structure of clays.

Keywords: clay; in-situ polymerization; metallocene; modeling; nanocomposite; Polyolefins; support

Introduction

Polyolefin-clay nanocomposites are a new type of polyolefin-based composites that can provide much better physical properties than those of conventional composites. The clays commonly used in nanocomposites belong to a structural family known as 2:1 phyllosilicates. Their crystal layers are composed of a central alumina or magnesia octahedral plane fused to two silicate tetrahedron sheets, in a way that the oxygen atoms are part of the silicate tetrahedrons. The total layer thickness is about 1 nm and the lateral dimensions vary from around 300 nm to several micrometers, depending on the type of layered silicate [1]

Isomorphic substitution within the layers, for instance replacement of Al^{3+} by Mg^{2+} or of Mg^{2+} by Li^{+}, causes an imbalance of electrostatic forces generating residual negative charges on the surface of the layers (Figure 1, bottom side). The spaces between layers are called *galleries* or *interlayers*. The surface charges within the galleries are counterbalanced by cations such as Na^{+}, which are located inside the galleries. A typical clay particle is composed of many of these layers stacked together in an assembly called a *tactoid*.

In nature, layered silicates are found as rocks or powder, with micron-sized flaky particles, as shown in Figure 2. The typical dimension of clay particles found in powders varies from 10 μm to 0.1 mm. Each of these particles are agglomerates of smaller, flaky particles with dimensions varying from 1 to 10 μm. These particles will be called macroparticles in our mathematical model. Each macroparticle is itself

Chemical Engineering Department, University of Waterloo, 200 University Av. W., Waterloo, Ontario, Canada, N2L 3G1
E-mail: lsimon@uwaterloo.ca

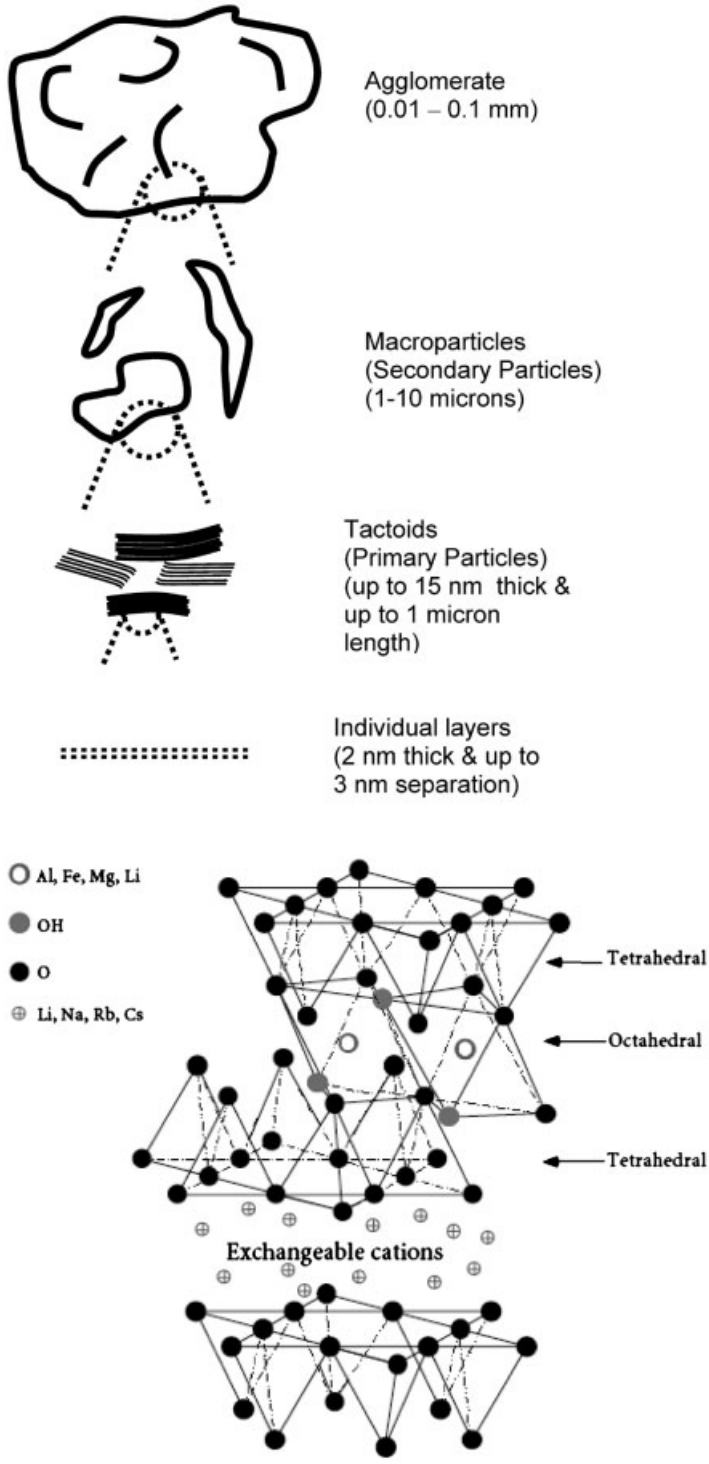

Figure 1.
Structure hierarchy (top side) and generic structure (bottom side) of layered silicates.[1]

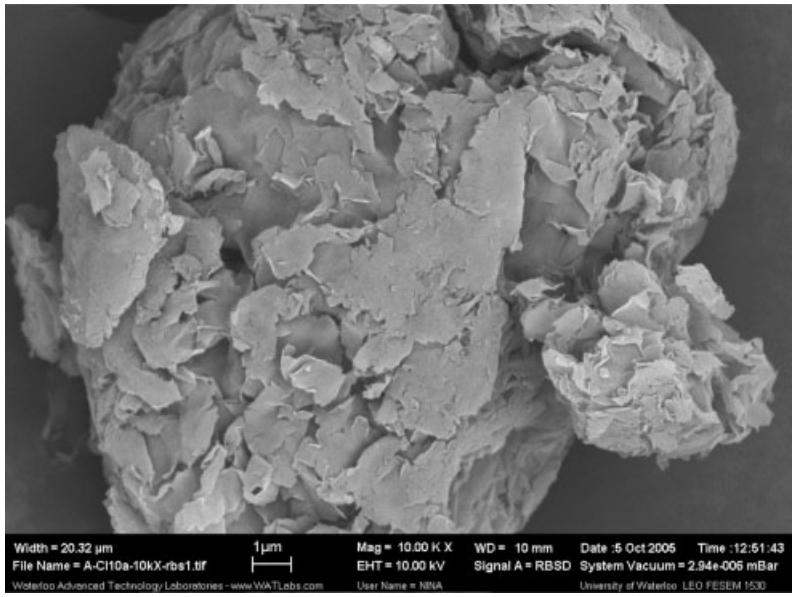

Figure 2.
SEM image of a clay (montmorillonite) particle, with 10,000x magnification.

composed of several tactoids several nanometers thick and up to a micron in length. A summary of structural hierarchy of the clay particles is shown in the left side of Figure 1 (top side).

Usually, clays used in the production of nanocomposites are subjected to an ion-exchange treatment in which small cations are substituted with larger and weaker cations such as quarternary alkyl ammunium ions to make them more hydrophobic. The advantages of this treatment is twofold: it increases the compatibility between the clay surface and the polymer phase and also widens the interlayer spacing between the clay platelets, favoring the diffusion of polymer chains during the intercalation and exfoliation steps.

There are two main methods for polyolefin/clay nanocomposite production: melt processing and in-situ polymerization. The main objective of these techniques is to separate and disperse the nanolayers as much as possible in the polymer phase. In the in-situ polymerization technique, the catalyst sites are supported on the clay and polymer is produced directly between the clay galleries; as a consequence, the growing polymer chains separate and disperse the layers in the polyolefin matrix. Melt mixing, as the name indicates, involves the physical mixing of polymer and clay phases. To be effective, the clay has to be organically modified to ensure good compatibility between the organic and inorganic phases.

The multigrain model (MGM) is on of the most commonly used models to describe particle fragmentation and polymer growth in heterogenous polymerizations coordination catalysts, either with Ziegler-Natta catalysts or supported metallocene catalysts[2]. In this model, each catalyst particle (macroparticle) is considered to be composed of a large number of smaller particles (microparticles). Active sites are supposed to be present at the surface of the microparticles. Monomer molecules diffuse through the pores of the macroparticle and the polymer layer surrounding the microparticles to react at the surface of the microparticle.

The model we are proposing is an extension of the MGM to model polymerization of olefins with catalysts supported on clay. In this case, the active sites are not supported on the surface of the microparticles, but instead are located inside the clay galleries. Therefore, before exfoliation takes place destroying the ordered structure of clay nanolayers (exfoliation), monomer has to diffuse through these galleries (nanolayered geometry). Figure 3 illustrates a schematic of our proposed model, called multilayer model (MLM).

On the left side of the Figure 3, the primary and secondary particles are shown, together with a typical radial profile for monomer concentration ($C \times r$). On the right side, the morphological change of clay layers from a tightly packed tactoid (before polymerization) to a random distribution of single layers (exfoliation after polymerization) is presented. Each primary particle can be composed of more than one tactoid but, for simplicity, just one tactoid is shown for each primary particle in Figure 3.

This modification of the MGM is necessary to account for the different morphology of the support. The mechanism for particle growth and fragmentation commonly associated with the MGM requires another level of hierarchy to account for the layered structure of the tactoids. When clay is used as a support, particle growth has to account for exfoliation if a nanocomposite is to be obtained. The current MGMs available in the literature are not meant to consider exfoliation. Furthermore, it is well known that the MGM is only approximate for spherical particles, so for clay particles it will be even less appropriate. Thus the model proposed here expands the MGM by adding the tactoid (layered) structures. The tactoids are considered as layered discs (for lack of better form) and the final clay particles are considered as spherical particle.

Interlayer Polymerization: Model Description

As a natural material, the single layers in Montmorillonite have irregular geometry. The model assumes the single layers to have disc geometry; it is a reasonable initial approximation and it provides convenient symmetry, simplifying the model. Accord-

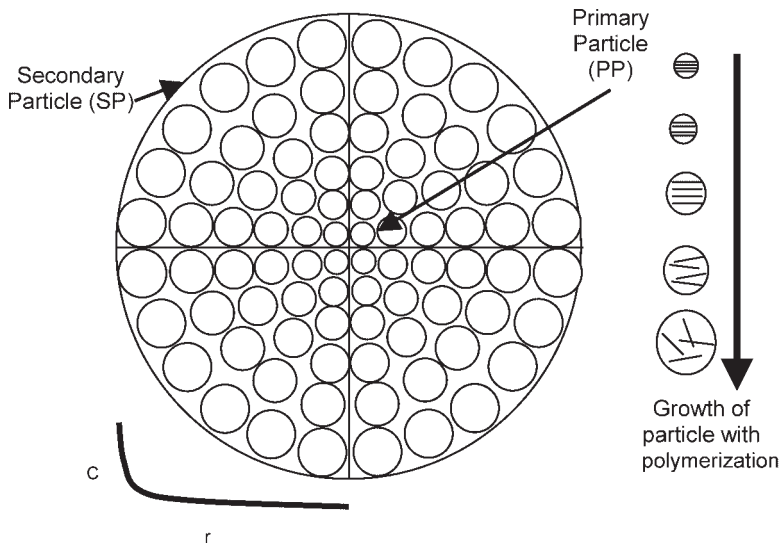

Figure 3.
A schematic of the modified multigrain model (multilayer model – MLM).

ing to our model, to reach the active sites located inside the clay galleries, monomer in the secondary particle must reach the opening of the gallery and diffuse radially towards its centre.

Individual clay layers are modeled as discs (Figure 4) with given radii, R, initial gallery spacing, h, and catalyst concentration, C. The galleries are surrounded by monomer in the secondary particle with concentration, M_b.

The normalized partial differential equation for diffusion and reaction in cylindrical coordinates is,

$$\frac{\partial M}{\partial t'} = \frac{1}{r'}\frac{\partial}{\partial r'}\left(r'\frac{\partial M}{\partial r'}\right) - \frac{R^2}{D}R_v \quad (1)$$

where M is the monomer concentration inside the gallery, D is diffusion coefficient inside the gallery, and

$$r' = r/R \quad (2)$$

where r is the radial position on the cylindrical coordinates and

$$t' = t \cdot {}^{D}/_{R^2} \quad (3)$$

The term R_v is the polymerization rate per unit volume, given by,

$$R_v = k_p \cdot M \cdot C \quad (4)$$

where k_p, M and C are the propagation constant, monomer concentration, and concentration of active sites in position r and time t.

Equation (1) is subjected to the following boundary and initial conditions:

$$M(r' = 1, t') = M_b \quad (5)$$

$$\frac{\partial M}{\partial r'}(r' = 0, t') = 0 \quad (6)$$

$$M(r', t' = 0) = 0 \quad (7)$$

Equation (1) was solved using Euler method (explicit finite differences).

The following assumptions were made in the model:

a. Isothermal polymerization
b. Uniform catalyst distribution inside the gallery
c. Monomer concentration (i.e., in the secondary particle) is constant outside the clay layers

Assumption (b) was made based on the average catalyst concentration obtained experimentally. Although the assumption of uniform catalyst concentration may not be a good one, it is a simple one and provides a starting point for the modeling work. Note that the catalyst concentration assumed here (Table 2) is too low to provide uniform distribution of active sites in all galleries. For modeling purposes such limitation can be addressed by simply increasing the catalyst concentration or assuming non-uniform catalyst distribution in the galleries. The authors are currently working on experiments that will contribute

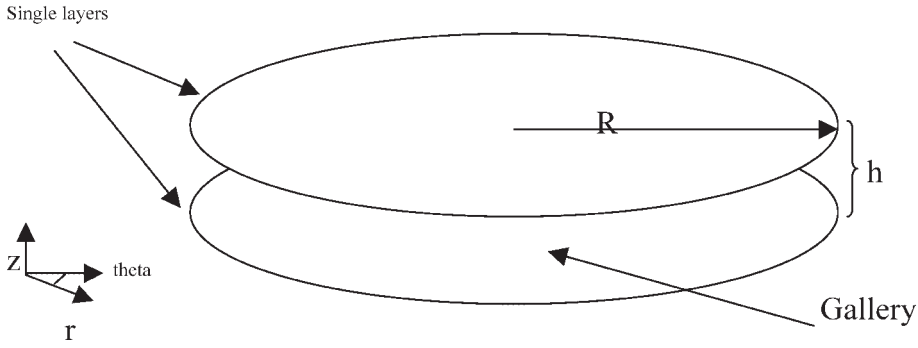

Figure 4.
Model for a clay gallery.

to model validation. Assumption (c) was made just to solve the problem at the clay gallery scale. In the next version of the multilayer model (MLM), this hypothesis will be relaxed to account for mass transfer effects in the macroparticle. Presently, we are only interested in understanding the exfoliation phenomena that takes place as polymer is formed between the clay galleries.

The polymerization takes place in a constrained geometry and there is no clear image of how the gallery is filled with polymer or how the layers are exfoliated. Therefore, as a first approximation, we assumed that as polymer is produced on the active sites, it does not "flow" either outside the gallery or to other adjacent positions in the gallery. As the volume of the produced polymer exceeds the volume between two clay layers, the gallery starts to expand (exfoliate). Because of the constant number of active sites supported on the clay surface and the increasing polymer volume, the local concentration of the catalyst (inside the gallery) decreases during expansion. A schematic of this mechanism is shown in Figure 5. Below each gallery, a typical monomer concentration profile is sketched. According to this picture, as the polymerization proceeds, the monomer concentration profile becomes increasingly more uniform.

By having this image of the clay exfoliation process, Equation (1) is discretized using explicit finite difference (Euler) method as explained below. If we select n as number of nodal points used to discretize the gallery, then:

$$\Delta r' = \frac{1}{n-1} \tag{8}$$

The time interval $\Delta t'$ is selected to ensure the solution is stable.

For a typical i^{th} element $(1 < i < n)$, the finite difference form of Equation (1) becomes:

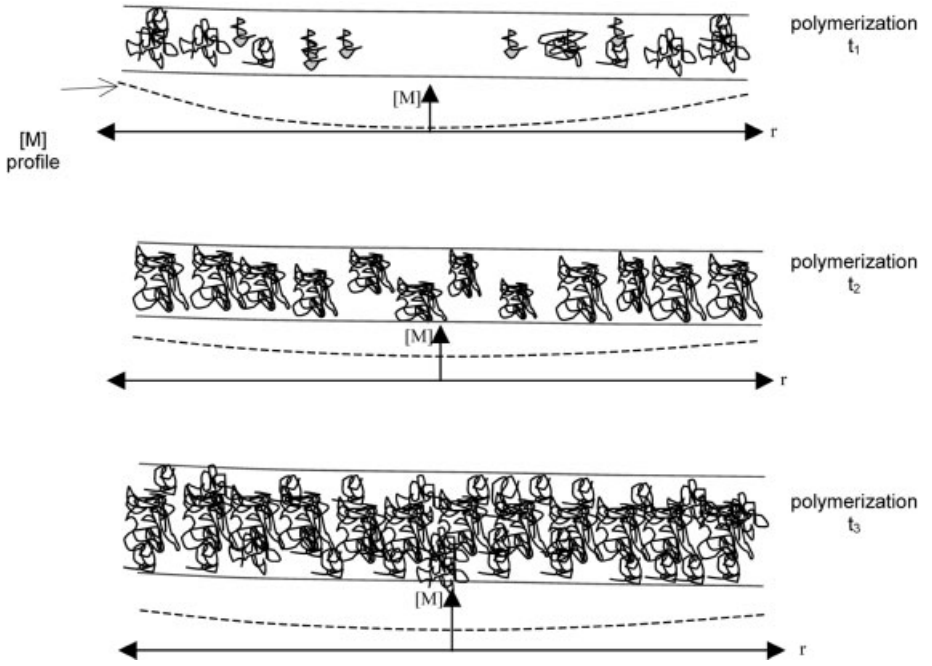

Figure 5.
Schematic cross section of single gallery formed by two discs showing separation of layers due to expansion caused by polymerization. Monomer concentration profile inside the gallery is shown below each gallery (dashed lines). Polymerization times $t_1 < t_2 < t_3$.

For $i = n$ (gallery edge), the monomer concentration is assumed to be M_b

$$M(i,t'+1) = M(i,t') + \Delta t' \cdot \left[\frac{1}{r'} \cdot \left(\frac{M(i,t') - M(i-1,t')}{\Delta r'} \right) + \left(\frac{M(i-1,t') - 2M(i,t') + M(i+1,t')}{(\Delta r')^2} \right) - \frac{R^2}{D} K_p \cdot C(i,t') \cdot M(i,t') \right] \quad (9)$$

$$M(n,t'+1) = \text{constant} = M_b \quad (10)$$

and for $i = 1$ (gallery centre), for any time including t'+1:

$$M(1,t'+1) = M(2,t'+1) \quad (11)$$

Results and Discussion

In order to represent different polymerization conditions and evaluate their effect on the final result of polymerization inside the gallery, we changed the propagation rate (k_p) and monomer diffusion coefficient (D) in the model. The range considered for these parameters are shown in Table 1.

Other model parameters are listed in Table 2. These values were selected based on the common and available ranges for reaction parameters[3,4], monomer diffusion rate[4] in the polymer and nano-layer geometries.

The two main outputs of the model are the gallery expansion profile and the monomer concentration profile inside the gallery. This capability will be initially exemplified here for a 10-minute polymerization with $k_p = 1 \times 10^8$ cm^3/mol.sec, $D = 1 \times 10^{-8}$ cm^2/sec and initial gallery spacing = 0.5 nm. Figure 6 shows that the monomer concentration decreases slightly from the opening to the center of the gallery, following the common trend for reaction-diffusion examples in porous media. Despite the high propagation rate constant ($k_p = 1 \times 10^8$ cm^3/mol.sec) and low diffusion coefficient ($D = 1 \times 10^{-8}$ cm^2/sec), the monomer concentration gradient is still very flat. This is mainly because of small diffusion time constant ($R^2/D = 1 \times 10^{-2}$ sec) for diffusion-reaction in typical clays.

Figure 6 also shows the interlayer expansion profile after 10 minutes of polymerization. Not surprisingly, since the monomer profile was quite flat for these simulation conditions, the separation between clay layers is also not a strong function of radial position. At the end of given time (10 minutes for the simulation in Figure 6) the volume percent of clay in the nanocomposites can be calculated. Using this information we can adjust the polymerization time to yield a desired polymer to clay ratio (volume percentage), also called clay content in the nanocomposite. In this case the calculated volume percent of clay is 74.8%.

The effect of propagation rate constant is shown in Figure 7. As expected, as the polymerization rate constant increases, the clay content in the nanocomposites decreases for the same polymerization time (1 minute). More interestingly, Figure 7 shows that down to $D = 1 \times 10^{-8}$ cm^2/s,

Table 1.
Range of parameter changes in interlayer polymerization.

k_p (cm^3/mol.s)	$1 \times 10^7 - 1 \times 10^{11}$
D (cm^2/s)	$1 \times 10^{-8} - 1 \times 10^{-5}$

Table 2.
Constants applied for interlayer polymerization.

M_b (mol/cm^3)	4.5×10^{-5}
C (mol/cm^3)	1×10^{-8}
h (Å)	5
R (nm)	100

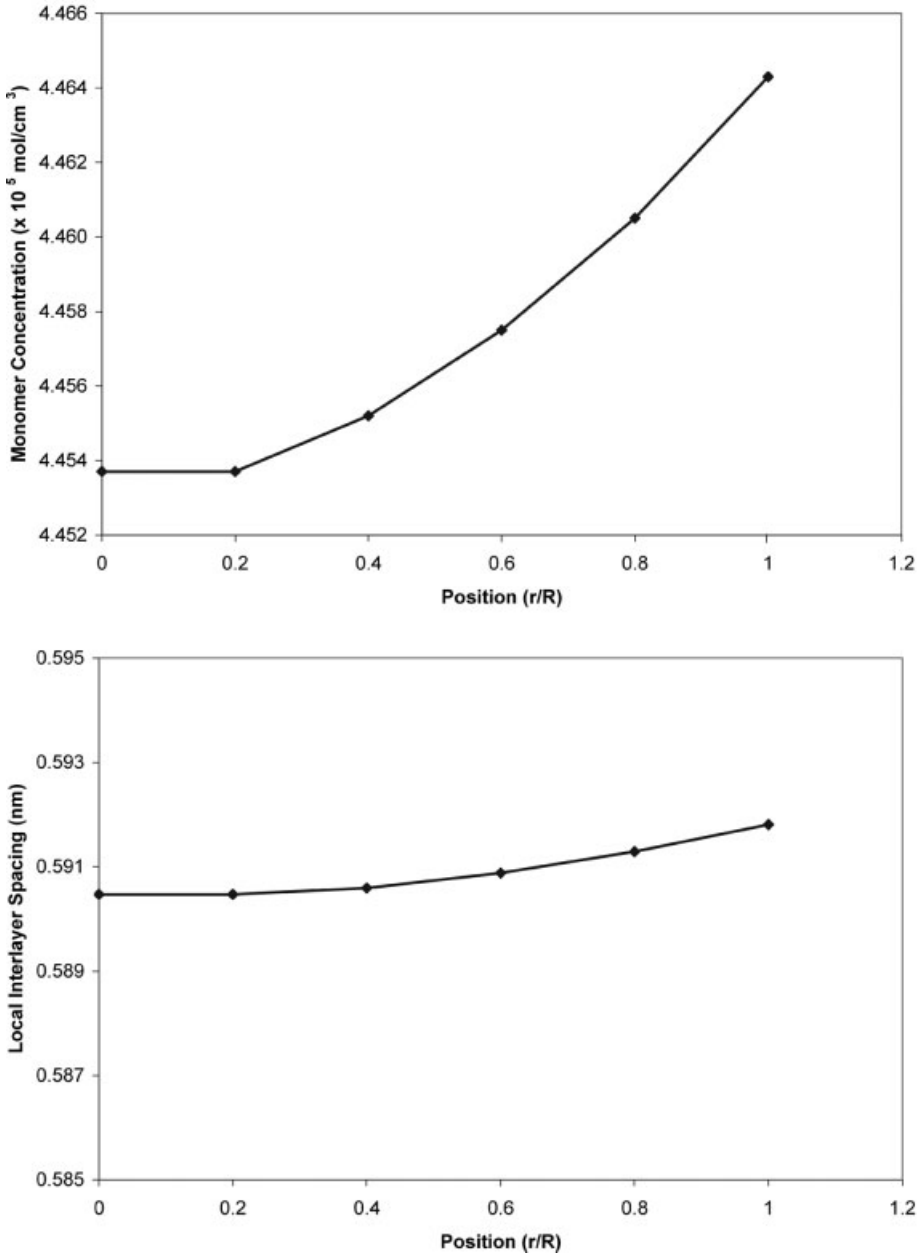

Figure 6.
Monomer concentration profile (top) and layer spacing profile (bottom) and vs. radial position (r/R) after 10 minutes of polymerization. Model parameters: $k_p = 1 \times 10^8$ cm^3/mol.sec, $D = 1 \times 10^{-8}$ cm^2/sec, clay content = 74.8%v.

the diffusion coefficient has a negligible effect on the polymerization. However, a further decrease in the diffusion coefficient will lead to monomer starvation and decrease the polymer content in the nanocomposite.

Regarding the effects of diffusion coefficient, as we see in Figure 7, decreased diffu-

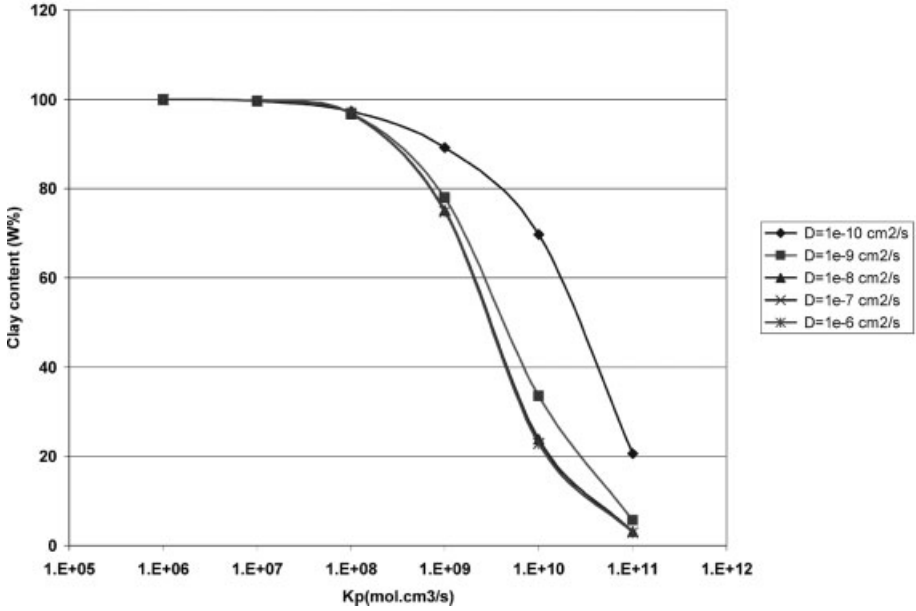

Figure 7.
Influence of the propagation rate constant on the nanocomposites clay content for several diffusivities. Polymerization time: 1 minute; other conditions given in Table 2.

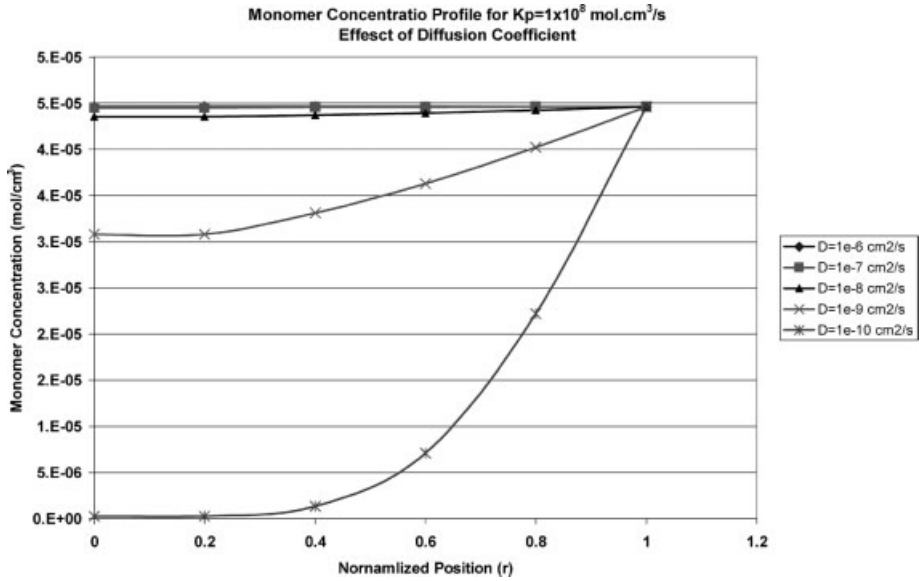

Figure 8.
Effect of diffusion coefficient, on the monomer concentration profile. Parameters values are: ($[C^*] = 1 \times 10^{-8}$ mol/cm^3, $[Mb] = 4.46 \times 10^{-5}$ mol/cm^3 , $D = 1 \times 10^{-6} - 1 \times 10^{-10}$ cm^2/sec, $K_p = 1 \times 10^{7} - 1 \times 10^{11}$ cm^3/mol sec, Thickness = 5 Angstrom (0.5×10^{-7} cm) , Disk Radius, R = 100 nm ($1 \times ^{-5}$cm)) on nanocomposites clay content. Polymerization time: 1 minute.

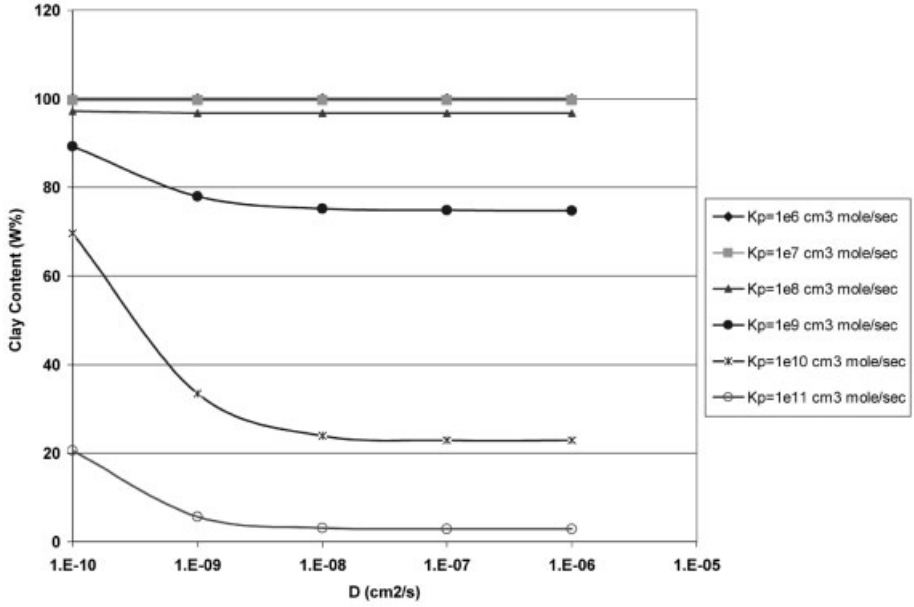

Figure 9.
Effect of diffusion coefficient, for ($[C^*] = 1 \times 10^{-8}$ mol/cm^3, [Mb] = Pressure (atm)/22400 mol/cm^3 , $D = 1 \times 10^{-5} - 1 \times 10^{-8}$ cm^2/sec, $K_p = 1 \times 10^7 - 1 \times 10^{11}$ cm^3/mol sec, Thickness = 5 Angstrom (5×10^{-7} cm) , Disk Radius, R = 100 nm ($1 \times ^{-5}$cm)) on nanocomposites clay content. Polymerization time: 1 minute.

sion coefficient causes steeper profiles in monomer concentration inside the gallery and therefore results in decreased total polymer production inside the gallery. Figure 8 shows the effect of diffusion coefficient on the monomer concentration profile.

In Figure 9, we can see that in relatively small polymerization rates, diffusion coefficient is not determining, but for higher polymerization rates (1×10^9 cm^3/mol sec) diffusion coefficient will be more significant. Below a $D = 1 \times 10^{-9}$ cm^2/sec (apparently not accessible) polymer production will be reduced drastically.

Conclusions

In order to use the multigrain model (MGM), we created a reaction-diffusion model to simulate the monomer diffusion into gallery spacing, polymerization yield (clay content) and interlayer expansion (exfoliation). The model is useful to explain the possible behaviors in clay exfoliation under different conditions. Although it is very early to make conclusions, this model predicts that the uniform distribution of catalyst inside the gallery and appropriate polymerization conditions should lead to steady polymer intercalation with subsequent exfoliation.

For better insight, this model will be expanded to the macroparticle level and validated with experimental results. Geometric variables such as average layer dimensions, gallery spacing, powder porosity and diffusion path tortuosity will be studied using this model to simulate the clay particle morphology.

[1] E. P. Giannelis, R. Krishnamoorti, E. Manias, *Adv. Polym. Sci.* **1999**, *138*, 107.
[2] T. F. McKenna, J. B. P. Soares, *Chem. Eng. Sci.* **2001**, *56*, 3931.
[3] J. Debling, W. H. Ray, *Ind. Eng. Chem. Res.* **1995**, 34, 3466.
[4] U. P. Veera, *Polym. React. Eng.* **2003**, *11*(1), 33.

